Surface roughness and directional fatigue behavior of as-built EBM and DMLS Ti6Al4V

SURFACE ROUGHNESS AND DIRECTIONAL FATIGUE BEHAVIOR OF AS-BUILT EBM AND DMLS Ti6Al4V

G. Nicoletto[a], R. Konečná[b], M. Frkáň[b], E. Riva[a]

[a]*University of Parma, Parco Area delle Scienze 181/A, Italy*

[b]*University of Zilina, Univerzitna 1,01026 Zilina, Slovakia*

Keywords: Ti6Al4V, powder bed fusion PBF, DMLS, EBM, fatigue, surface roughness, anisotropy

ABSTRACT

The powder bed fusion PBF is used in the fabrication layer-by-layer of metallic parts directly from a CAD file. Localized powder melting is obtained by a concentrated energy source, typically a laser beam or an electron beam. Fatigue tests of PBF Ti6Al4V were performed on smooth specimens produced with different orientations with respect to build direction using either a laser beam system (DMLS) or an electron beam system (EBM). As-built specimen were subjected the fatigue loading to understand and quantify the influence of the surface roughness and morphology. The original results are discussed on the basis of previous studies on the same material and processes taken from the literature.

1. INTRODUCTION

Powder Bed Fusion (PBF) is a denomination combining different additive manufacturing technologies that makes it possible to produce metallic components directly from a computer-aided design file of the part, [1]. PBF involves the same basic process where the material is fabricated layer-by-layer through localized melting and solidification of a metallic powder bed by a concentrated energy beam. The energy sources involved in PBF are either a laser beam or an electron beam. The laser-based technology is the most commonly used today and is associated to additional acronyms such as Laser Beam Melting (LBM), Selective Laser Melting (SLM), or Direct Metal Laser Sintering (DMLS) etc. Here the DMLS acronym will be used because the processing system used was produced by EOS GmbH, Germany. The EBM acronym will be used when referring to the electron beam processed material with the system by ARCAM AB, Sweden.

The EBM and the DMLS processes result in significant differences of the material structure, quality and performance, [2]. For example, the residual stresses in EBM parts are limited or absent as EBM is performed in vacuum at elevated temperatures, while the DMLS process, being generally performed in an inert gas environment with a non-heated building chamber, results in significant residual stresses that typically require a post stress relieving heat treatment.

The PBF technologies, i.e. both DMLS and EBM, can process a wide variety of metallic alloys, such as titanium, nickel, Co-Cr, aluminum and steels, [1]. Ti6Al4V is the most widely used titanium alloy because it features good machinability and excellent mechanical properties. The Ti6Al4V alloy offers the best all-round performance for a variety of weight reduction applications in aerospace, automotive and marine equipment. Ti6Al4V also has numerous applications in the medical industry because its biocompatibility is excellent, [2].

Despite the attractiveness of the unique design freedom offered by the PBF technology and the widespread use of conventional Ti6Al4V in the aerospace sector, several challenges hinder the application and certification of PBF Ti6Al4V parts for load bearing applications, [3-5]. The demanding reliability requirements of conventional Ti6Al4V parts, including fatigue validation by testing, apply to PBF Ti6Al4V parts.

The complexity of the set up and optimization of the PBF manufacturing process may negatively impact the fatigue performance of a part and have been under intense investigation,

namely i) the presence of internal defects, [6-10], ii) the residual stresses due to melting and solidification inherent to the process iii) the material microstructure obtained directly and its modification by post-processing heat treatments, [11], and iv) the as-built surface quality, which can be modified in principle by machining and/or finishing techniques, [12-15]. A short overview of the current understanding about these different aspects will be now given although the present contribution is essentially aimed at addressing point iv) because considered of utmost importance. As a matter of fact, the industrial practice and fabrication systems after process parameter optimization should result in a nearly fully dense material, absence of residual stresses eliminated by a post fabrication heat treatment that optimizes the microstructure in terms the static mechanical properties.

Two types of possible internal defects are typically identified in PBF metals: pores and voids. Pores are spherical with diameters on the order of the powder size used in the AM process. The shape and size of these pores indicates gas entrapment as the formation mechanism. Pores are considered by many to be unavoidable by-products of PBF metal processes. Voids are irregular in shape and tend to exist within one layer: their size is critical in defining their negative impact. A Hot isostatic pressing (HIPing) treatment is often adopted with the aim of closing stress-concentrating internal porosity and voids to improve fatigue endurance, [10, 13, 15]. However, HIPing induces microstructural changes besides residual stress relief. A reduction in tensile strength and yield stress with limited improvement in ductility with respect the heat treated material is reported in [13]. Its effectiveness in terms of fatigue improvement is apparently limited if the surface is in the as-built condition, [13, 16].

To assess the fatigue performance of PBF Ti6Al4V in comparison to conventionally produced (i.e. cast or wrought) Ti6Al4V, the common approach in the literature has followed the following steps: i) manufacture cylindrical or prismatic blanks, ii) heat treat the blanks (i.e. not only stress relieving but frequently also HIPing) and iii) machine blanks to obtain specimens of standard geometry, dimensions and surface finish (i.e. polish). The examination of published data revealed that the fatigue performance of PBF Ti6Al4V was superior to wrought and annealed Ti6Al4V because of the fine microstructure that can be achieved with PBF processing, [2]. However, this conclusion is true only when “well-prepared” specimens (i.e. surface finish, no residual stress, no internal defects) are used, [4].

While the expert PBF technologist can optimize the fabrication processes to achieve nearly theoretical material density, readily eliminate residual stresses and optimize the

microstructure, he cannot significantly control the as-built surface quality of the part surfaces once surface finishing or machining may not be desired or practical. Furthermore, the PBF part geometry is typically complex because geometrical complexity is possibly the strongest application driver. Therefore not only internal surfaces but also elaborated external surfaces may not be easily accessible for finishing and have to be left with the original as-built surface roughness. The resulting relatively poor fatigue strength is possibly the most significant acceptability challenge of the PBF technology when considered for the production of net-shape parts for load-bearing applications, [3,4,16].

As-built surfaces roughness is typically orders-of-magnitude larger than conventionally machined surfaces, [12, 17]. It depends on a complex combination of raw material quality (powder particle size), additive manufacturing system and processing parameters, surface orientation with respect to build direction etc., [7]. Several mechanisms, including stair-stepping, balling, and the formation of partially bonded surface particles have been identified to contribute to PBF roughness, [6,7]. Stair-stepping is the consequence of positioning errors of the energy source at the surface edge, the beam inclination angle and the slope of the surface edge being built. Balling and partially bonded surface particles are created when the heat on the border edge is not sufficient to fully sinter the particles.

Since the inter-relation between surface quality and fatigue is particularly important for the present work, a short overview of the role of as-built surfaces on fatigue behavior of DMLS Ti6Al4V and EBM Ti6Al4V is given now. While published studies typically considered either technology, here special attention will be also given to comparative studies, [16, 18]. The influence of process inherent surface roughness on fatigue performance have been investigated for TiAl6V4 [2-4,13, 14]. First of all the best demonstrated performance of specimens without surface treatment is less than traditional cast products. A significant lower endurance limit for smooth specimens with inherent surface roughness compared to polished ones for PBF specimens. Comparative studies [16, 17] have also reported a lower endurance limit for electron beam melted TiAl6V4 compared to laser melted TiAl6V4. The key role of post fabrication heat treatment on the fatigue endurance of laser powder bed melted specimens has been established [2, 3].

Since most fatigue studies adopted the standard cyclic tension specimen configuration, only the loading direction parallel to the build direction has been investigated for the as-built surface condition because other specimen directions would have required surface

modification after specimen removal from the build plate. The layer-by-layer processing of Ti6Al4V is however known to introduce a columnar grain structure with long axis parallel to build direction, [6, 19]. This feature could result in direction-dependent fatigue behavior.

Only a few studies investigated the combined effect of directionality of specimen fabrication and as-built surfaces on the fatigue behavior of PBF Ti6Al4V, [20, 21]. A mini specimen geometry was proposed in [20], for the ready fabrication of the differently oriented specimens with respect to build direction. The loading direction parallel to the build direction showed a significantly lower performance compared to other two loading directions investigated under plane cyclic bending. The novel experimental method of [20], already validated by comparison against standard rotating bending test results, is adopted here to develop a detailed comparison of the directional fatigue behavior of DMLS Ti6AL4V after an optimized heat treatment in vacuum and the fatigue behavior of EBM Ti6AL4V. The comparison in fatigue performance of the two technologies is compounded by the investigation of the original as-built surfaces and their respective morphology. The present results are corroborated by comparison with recently published fatigue test results using different geometry and test method.

2. EXPERIMENTAL DETAILS

2.1 Material and fabrication processes

The metal powder used in the present study was a certified titanium alloy Ti6Al4V ELI whose spherical particles were in the 25 to 45 μm diameter range. The specimen fabrication was carried out according to the DMLS process and the EBM process using two industrial systems and all DMLS and EBM specimens were built within the same jobs in the different systems to eliminate batch-to-batch scatter.

The DMLS system was an EOS M 290 (EOS GmbH, Germany) operating a laser of max 400 W power in a protective argon atmosphere with a process chamber temperature of 80 °C. The layer thickness was fixed to 60 μm. The scan strategy was according to the shell-and-core concept, with a specified fixed rotation of the laser hatching pattern between subsequent layer. After fabrication, the specimens were stress relieved according to the following thermal cycle:

heating up to 740 °C in a vacuum furnace, exposure for 2 h and slow cooling to 540 °C, followed by rapid cooling in Argon.

The EBM system was an ARCAM A2 (ARCAM AB, Sweden) operating in vacuum with the process chamber at 630 °C. The layer thickness was fixed to 50 μm. A shell-core scan strategy was used which alternates each layer between 0 and 90°. Differently to the DMLS process, no post fabrication heat treatment was required after separation from the build plate. The EBM process is based on a high power electron beam that generates the energy needed for high melting capacity and high productivity. As a result, the parts produced with the EBM process are almost free from residual stresses and have a microstructure free from martensitic structures.

Light optical microscopy was performed on both EBM and DMLS samples to determine the presence of internal defects. Metallography, optical and scanning electron microscopy (SEM) were applied for the characterization of the microstructure and of the surface quality.

2.2 Directional specimens and fatigue test method

Batches of mini specimens specifically oriented with respect to the build direction were fabricated to investigate the directional fatigue behavior of as-built DMLS Ti6Al4V and EBM Ti6Al4V. Fig. 1 schematically shows the three different orientations of the specimens on the build plate with respect to the build direction and the respective denomination. The smooth plane surface of the specimen is subjected to a cyclic bending tensile stress with a load ratio R = 0 (hence stress concentration factor K_t = 1). The white arrows of Fig. 1 show the applied stress direction and the imposed interaction of stress and the layer-by-layer material structure. In Type A specimen, the top layer is under highest stress, the stress in Type B specimen is parallel to the layers while the stress in the Type C specimen is perpendicular to the layers. All specimen surfaces are in the as-built state, the fatigue testing determines the directional contribution to the fatigue behavior. The size of the reference section is 5 x 5 mm^2 and the length of the specimen is 22 mm. A total of about 50 specimens were used in the present test program, about 25 specimens per fabrication process and, typically and 7 or 8 specimens per orientation. The relatively limited number per direction was defined as a compromise between desired representativeness and necessary testing time on two available testing machines.

Fatigue experiments were performed on two Schenk type testing machines modified to continuous monitoring of the applied load during the test under a constant displacement range. The apparatus applied cyclic bending tensile stress (R = 0) at a frequency of 15 Hz. Test were interrupted above 2 x 10^6 cycles, if specimen did not fail (i.e. run-out).

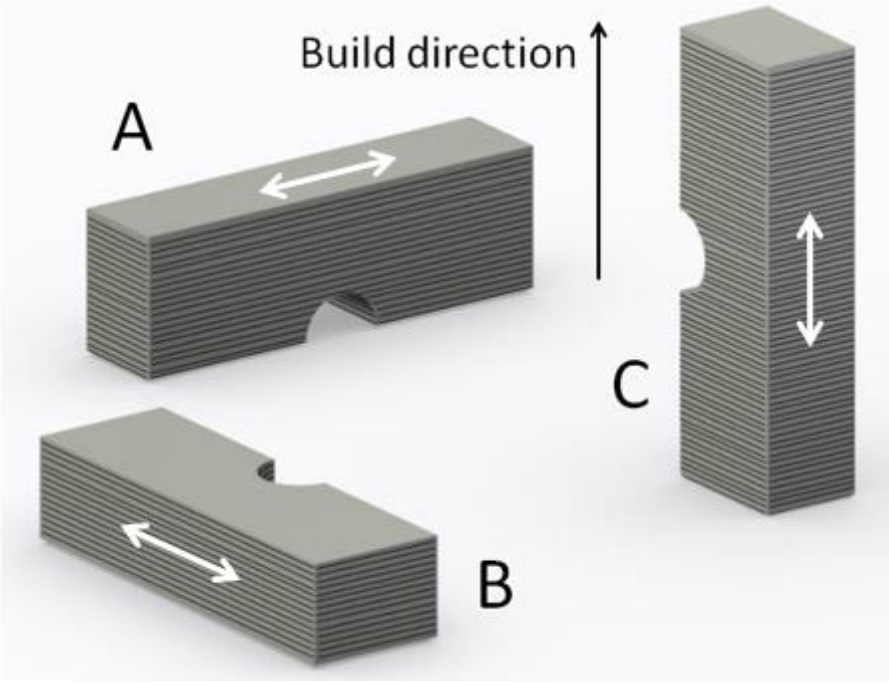

Fig. 1. Directional fabrication of fatigue specimens and denomination. White arrow defines the applied stress direction. The layer-by-layer construction is schematically shown.

2.3 Material microstructure

The EBM and DMLS processes involve quite different thermomechanical condition applied to the powder and the part. The microstructure is expected to dominate the fatigue performance only when the surface is machined and internal defects are very small or absent. Near theoretical densities are achieved with an optimized fabrication process. A HIP treatment is often advocated to eliminate even internal defects so small that their damaging role is questionable.

A metallographic investigation on polished and etched specimen sections using optical microscopy was carried out to identify structural differences between DMLS Ti6Al4V and EBM Ti6Al4V using a Neophot 2 microscope. Polished sections were etched with 10% HF.

Observations on three perpendicular planes were made. In general, the material produced by DMLS fabrication shows a finer microstructure than EBM technology. The microstructure on lateral planes of the DMLS material, Fig. 2a, is characterized by primary columnar β grains, well observed at low magnification which transformed during cooling from the stress relieving temperature of 740 °C to fine needles of α phase in β matrix, Fig. 2a. Fine lamellas of (α+β) phases were present in the EBM material, Fig. 2b. Widmansttäten basket wave microstructure is typical to both materials, Fig. 2c and 2d. The presence of α phase on boundaries of primary β grains was observed in case of EBM material, especially on perpendicular sections (i.e. x-y plane in Fig. 1), as shown in Fig. 2d. The temperature influences the coarseness of lamellar TiAl6V4.

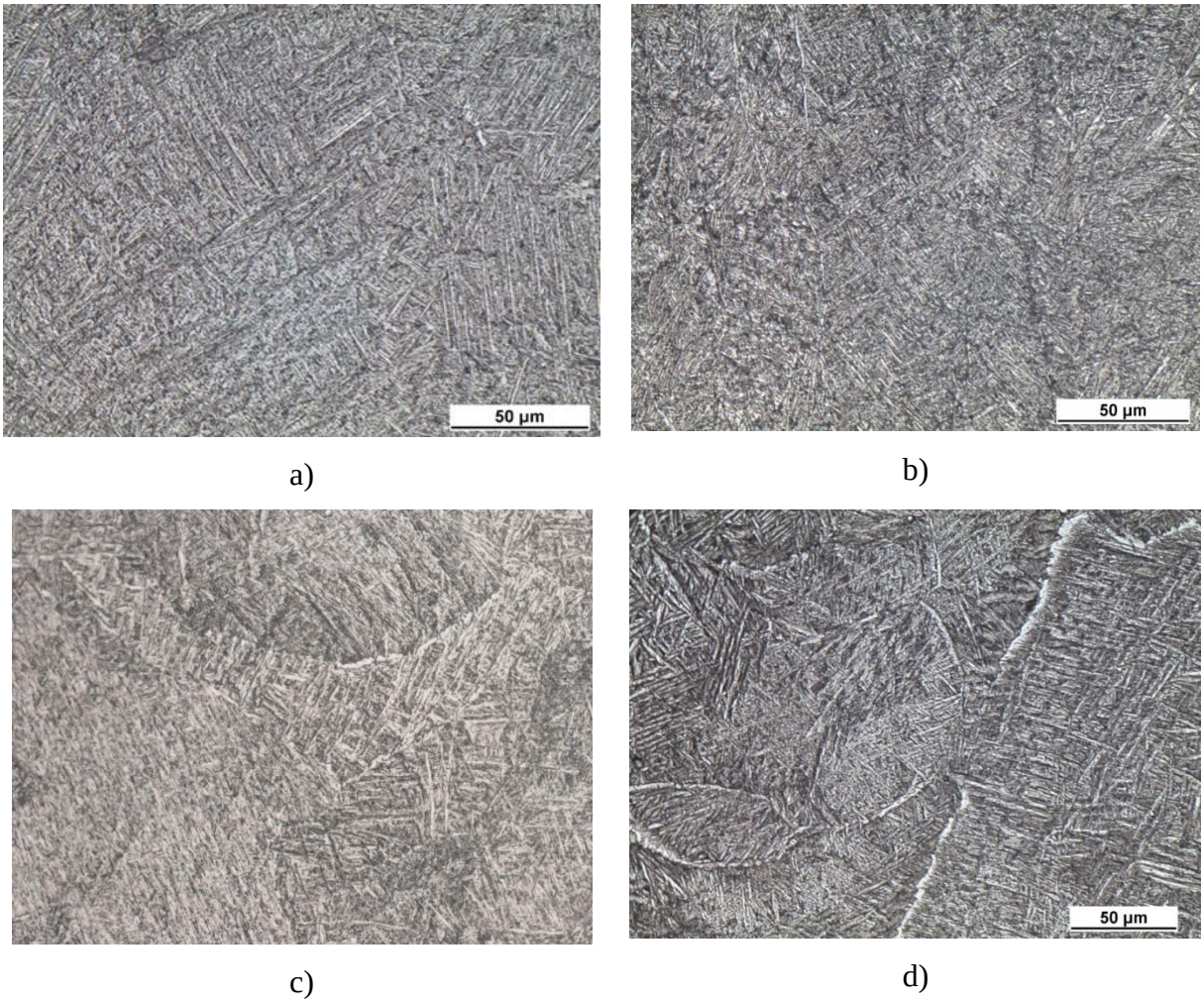

a) b)

c) d)

Fig. 2 Microstructure of Ti6Al4V on lateral planes a) and c) fine needles of α phase in β matrix, DMLS and perpendicular planes b) and d) fine lamellas of (α+β) phases, EBM; etched

10% HF, OM

2.4 As-built surface characterization

The two different technologies result in different surface quality. This is especially important when testing in fatigue specimens with as-built surfaces. Furthermore, considering the directionality of the present specimen fabrication scheme shown in Fig. 1, different surface quality are achieved on the surfaces under stress. Namely, the surface roughness is associated to the generation of the top layer in Type A specimen, while the surface roughness depends on its generation by subsequent orthogonal layers in Type B and Type C specimens. Now a qualitative examination of the as-built surfaces provides an insight of the link between PBF process and surface quality. Fig. 1 shows not only the direction of the applied cyclic stress but also the direction of the line scan for the roughness determination carried out with a Mitutoyo SJ 210 system.

Typical surfaces for the two PBF process were observed in the SEM and are shown in Fig. 3. Different image magnifications are used in Fig. 3 in dependence of the specific PBF process. Fig. 3a shows the flat as-built surface perpendicular to the build direction (i.e. Type A specimen) obtained by DMLS. Fig. 3c shows analogous surface obtained by EBM.

Instead, the surfaces under test of Type B and Type C specimens have their normal perpendicular to the build direction. Typical surfaces for the DMLS process and for the EBM are shown in Fig. 3b and 3d, respectively. In the case of DMLS production the as-built surface of Type A specimen, Fig. 3a, is almost flat while for Type C, Fig. 3b, is characterized by partially bonded surface particles on the layer border edges. In the case of EBM production, the plane of Type A specimen, Fig. 3c, shows a wavy character while for Type C, Fig. 3d, the surface is very rough. The surface texture is formed by a network of partially molten particles.

Fig. 3a and 3c are characterized by a regular and well defined pattern of solidified raster tracks (i.e. primary roughness) with limited powder entrapment. Fig. 3b show that on the lateral surfaces of DMLS specimens the fully melted layers define a primary roughness modulated by the layer thickness with a contribution of a secondary roughness of partially melted powder particles. Fig. 3d shows that on the lateral surfaces of EBM specimens the

roughness is a unique product of the melted layers with a grainy appearance and without evidence of a preferred direction.

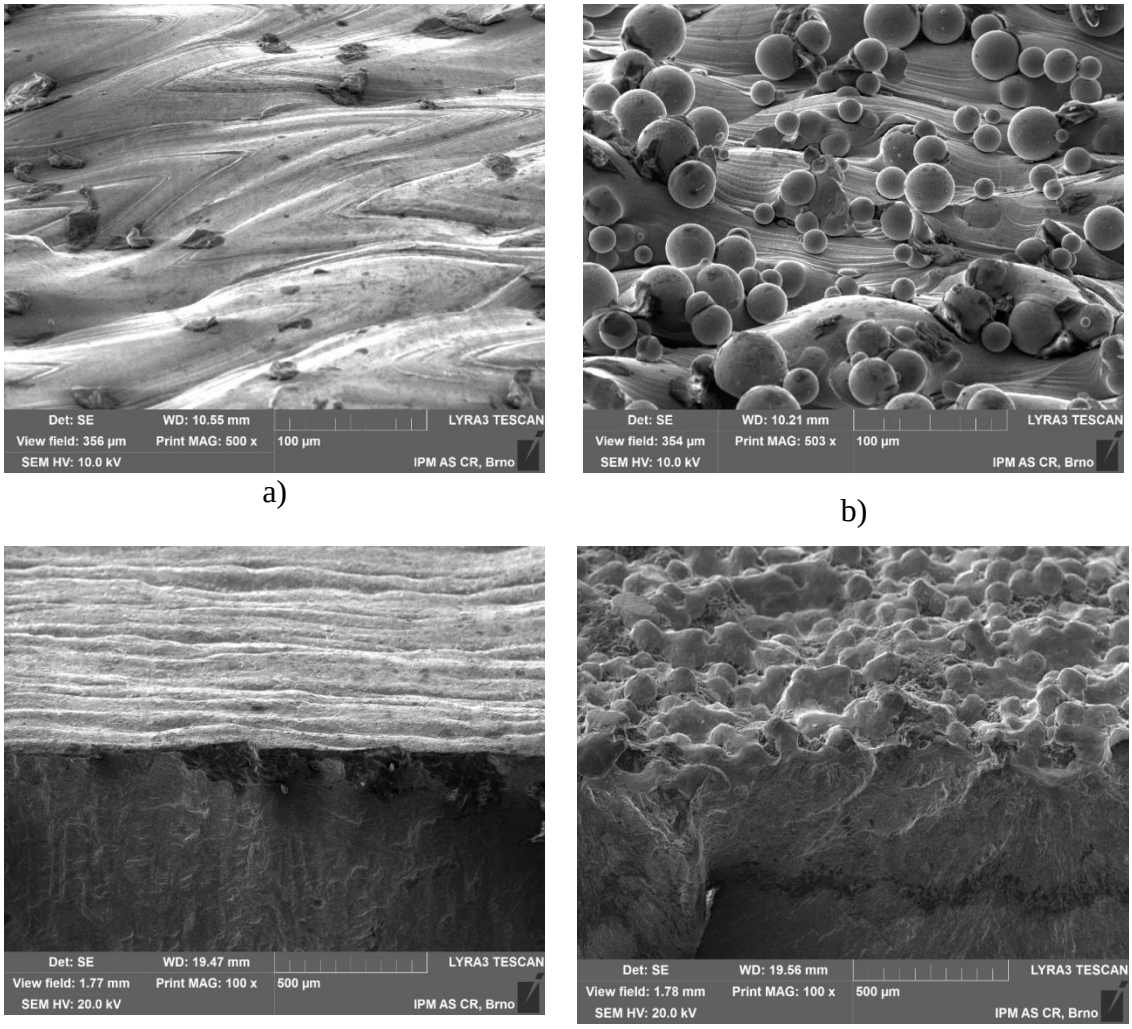

Fig. 3 As-built surface perpendicular to the build direction a) DMLS and c) EBM; as-built surface parallel to the build direction b) DMLS and d) EBM, SEM (please, note the different magnifications).

2.5 Reference static properties

Smooth specimens for tensile testing oriented in the build direction were included in the different print jobs for quality assurance purposes and followed the entire fabrication process

of the fatigue specimens. The tensile specimens were then tested and provided the following reference static mechanical properties.

For the DMLS Ti6Al4V after stress relief heat treatment, a tensile strength was R_m = 1176 MPa, yield stress was $R_{p0.2}$ = 1104 MPa and elongation to rupture was A = 12.9 %. For the EBM Ti6Al4V (i.e. no post fabrication heat treatment) the ultimate tensile strength was R_m = 1020 MPa, yield stress was $R_{p0.2}$ = 950 MPa and elongation to rupture was A = 14 %. These data for both PBF processes are in line with data reported in the literature, [3,4,16,18] and are all above the minimum specifications contained in the ASTM F2924 norm covering additively manufactured Ti6Al4V components using full-melt powder bed fusion such as electron beam melting and laser melting, [22]. These values are for parts that should have mechanical properties similar to machined forgings and wrought products.

The lower tensile and yield strength of the EBM Ti6Al4V compared to that of the DMLS Ti6Al4V was expected due to the process details given before. Differently to DMLS, during EBM processing the build chamber is kept at an elevated temperature throughout the entire build, and the material thus comes out of the EBM process in a naturally aged condition, [16]. The high temperature involved tends to decrease the yield and ultimate tensile strength and slightly increase the elongation to rupture.

3. RESULTS

3.1 Directional fatigue behavior of DMLS and EBM Ti6Al4V

DMLS Ti6Al4V

Fatigue test results of directional as-built Type A, Type B and Type C mini specimens of DMLS Ti6Al4V are shown in Fig. 4. The post fabrication heat treatment in vacuum applied in this study results a fairly isotropic response. However, if the directional data are connected with trend curves, a degree of anisotropy is identified and some comments can be made. Fig. 4 shows that Type C specimens are generally associated to slightly shorter lives while Type A specimens at high applied stress have the best performance and Type B slightly better at lower stresses.

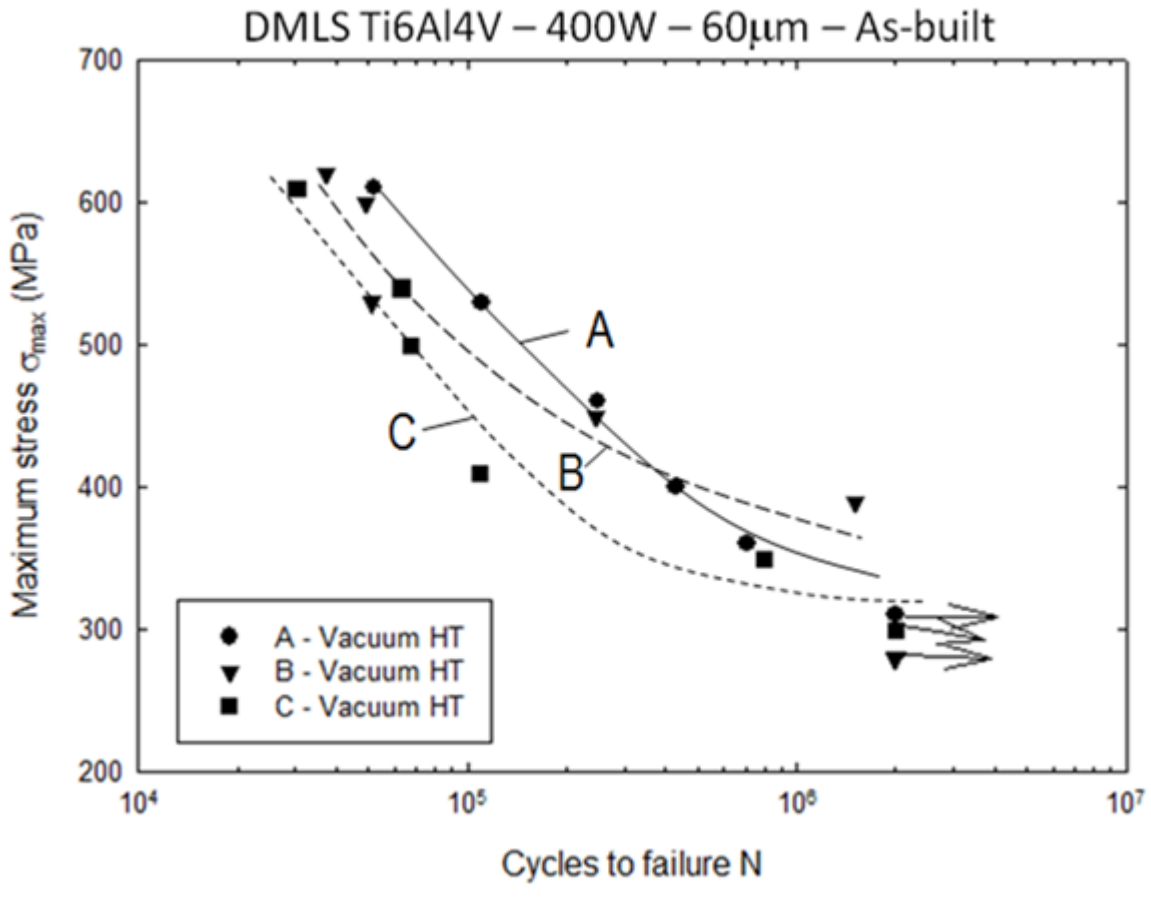

Fig. 4 Directional fatigue curves of as-built and heat treated DMLS Ti6Al4V (R=0).

This response is quite different from previous directional results on DMLS Ti6Al4V, [20], where type C specimens showed a significantly lower fatigue strength compared to the other two directions. The motivation is in the different post fabrication heat treatment of the two batches of DLMS Ti6Al4V that were significantly different in terms of heating temperature (i.e. 740°C x 2 hrs in this work, 380°C x 8 hrs in [20]). On the other hand, the present data are coherent with the results of [4] on the same DMLS alloy. A thorough discussion and comparison with other previous test results on the same material is given elsewhere, [20].

EBM

The fatigue test results of directional as-built Type A, Type B and Type C mini specimens of EBM Ti6Al4V are shown in Fig. 5. The EBM processing in vacuum and at high temperature results in a rather isotropic fatigue behavior of the directional mini specimens. Fatigue data are also well-behaved as in Fig. 4 for DMLS counterpart.

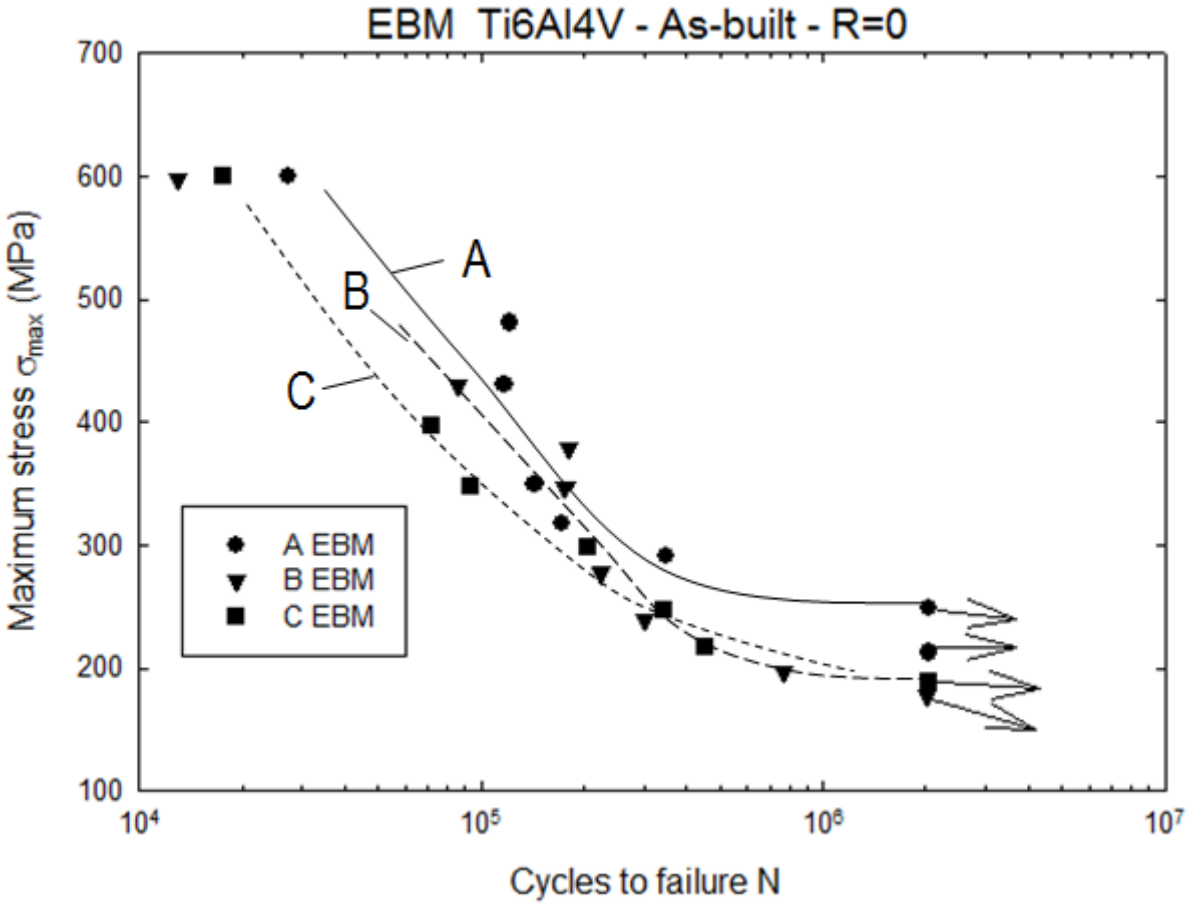

Fig. 5 Directional fatigue curves of as-built EBM Ti6Al4V (R=0).

Trend curves shows a slightly better performance of Type A specimens with run-outs at significantly higher stress than Type B and Type C specimens, which are indistinguishable. The directional effect agrees in this case with roughness measurements that show that Type A specimens have the lowest surface roughness of all directions.

DMLS vs EBM

The comparison of the fatigue performance of the two PBF processes is shown if Fig. 6. Considering the relative narrow scatter of the directional fatigue data of the previous Fig. 4 and 5, two trend curves including directionally-generated scatter bands are defined allowing a direct comparison of the global fatigue response of the two PBF processes applied to the same Ti6Al4V alloy.

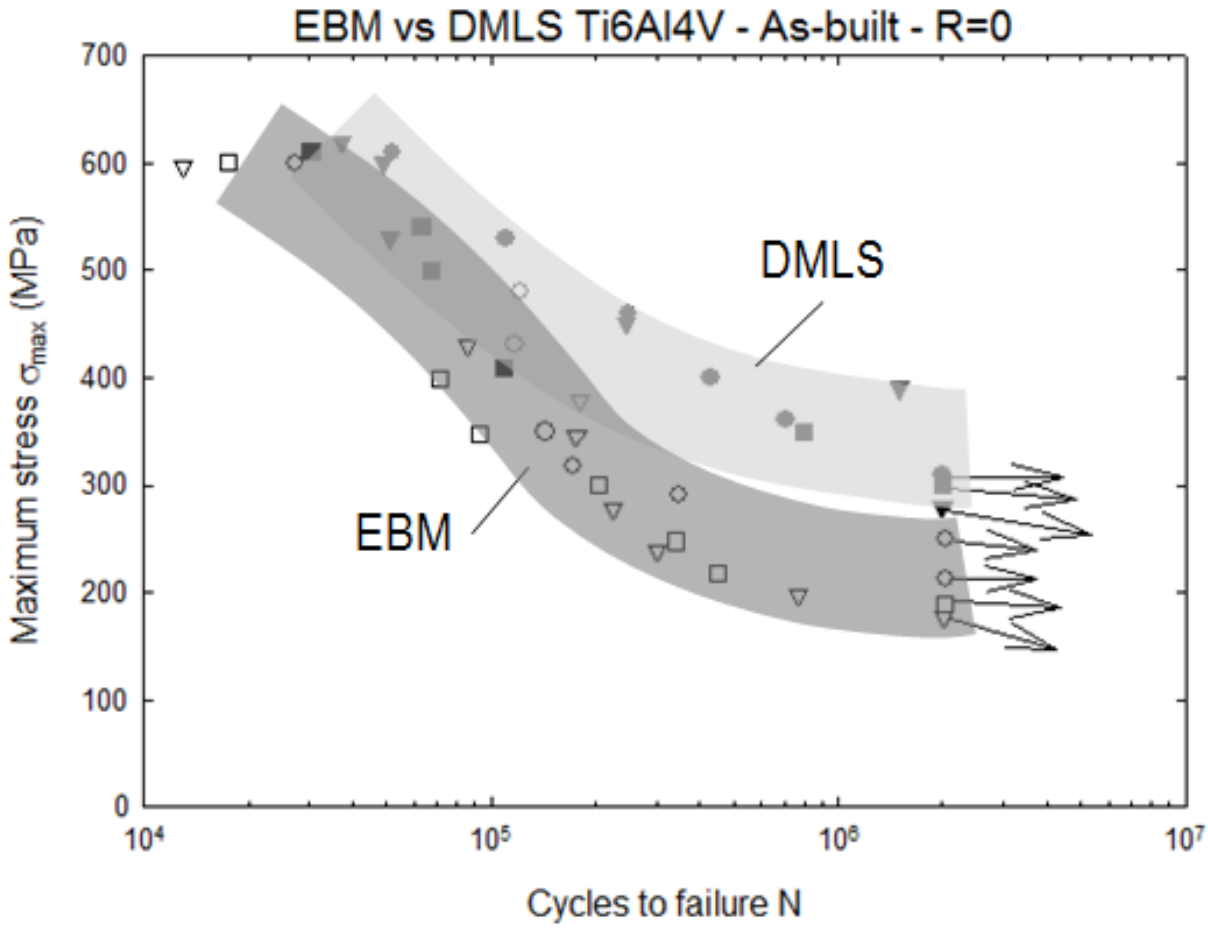

Fig. 6 Comparison of global fatigue curves of as-built EBM vs DMLS Ti6Al4V.

The fatigue response of the as-built DMLS Ti6Al4V is clearly better than that of the as-built EBM Ti6Al4V especially at long lives. On the other hand, the two scatter bands overlap locally at high applied stresses. The increment in as-built fatigue strength at 2 10^6 cycles of DMLS over EBM is estimated in about 50%. In the subsequent discussion, this data will be compared to previous findings in the literature.

A contributing factor may be given by the correlation between tensile strength and fatigue strength often assumed for many metals. As reported in a previous subsection, the present high temperature EBM processing of Ti6Al4V resulted in tensile strength and yield stress that are both lower than the corresponding values of DMLS-processed Ti6Al4V after post fabrication heat treatment.

Estimates of the bending fatigue strength at 2 10^6 cycles are extracted from the scatter bands of Fig. 6 and presented in Table 1 according to two possible definitions: i) in terms of

maximum stress σ_{max} (as now customarily done in the literature when testing is at R = 0 or 0.1) and ii) in terms of an equivalent stress amplitude $\sigma_{a,eq}$ using the Haigh mean stress effect conversion equation for transforming the present data at R=0 in the equivalent value for R=-1 loading condition, which is typical of rotating bending tests.

Tab. 1 Estimates of bending fatigue strengths at 2 10^6 cycles for as-built Ti6Al4V

Fabrication process	HT temperature and time	Maximum bending stress σ_{max} at R=0 (MPa)	Equivalent bending stress amplitude $\sigma_{a,eq}$ at R= -1 according to Haigh equation (MPa)
EBM	-	200 (Type A - 260)	110
DMLS	740°C x 2 hrs	320	184

Finally, it has to be considered that the previous values in Tab. 1 are nominal stresses in the net section of the specimen and overestimate of about 10% the actual tensile stress on the flat surface as determined in the elastic calibration presented elsewhere, [20].

3.2 As-built surface features of DMLS and EBM Ti6Al4V

In a previous subsection a qualitative description of the different as-built surfaces associated to the two PBF processes was given based on SEM images. Now a quantitative comparison of the surfaces is presented to support the discussion of the fatigue test results of this work. Roughness measurements of the different surfaces under the fatigue loading for the different specimen directions of Fig. 1 are presented in Tab. 2 for the DMLS Ti6Al4V and in Tab. 3 for EBM Ti6Al4V, respectively.

The roughness parameters considered are Ra and Rz because are the most widely used for quality control and often reported in the literature. Furthermore, this study is dedicated to the interaction of the applied stress and the as-built surface and the resulting fatigue strength. Therefore, the line scan for roughness in the direction of applied stress measures peaks and valleys affecting crack initiation.

A first observation of the results shows that, when the same specimen type is considered, the roughness of DMLS material is always lower than the corresponding roughness of EBM material. The two parameters Ra and Rz coherently confirm the differences.

Table 2 Surface roughness of the plane under fatigue loading, DMLS production

Roughness measure	Type A	Type B	Type C
Ra [μm]	3.3 ± 0	13.1 ± 0.3	13.4 ± 0.5
Rz [μm]	20.1 ± 3.3	88.8 ± 8.7	80.7 ± 8.2

Table 3 Surface roughness of the plane under fatigue loading, EBM production

Roughness measure	Type A	Type B	Type C
Ra [μm]	7.29 ± 2.85	17.05 ± 4.32	20.60 ± 3.9
Rz [μm]	41.66 ± 14.28	99.83 ± 23.86	126.05 ± 21.38

A second observation deals with the difference between the relative low surface roughness of Type A specimens compared to the higher surface roughness of Type B and Type C specimens for both the PBF materials. The roughness measurements support the qualitative visual assessment of the surfaces shown in Fig. 3. Finally, while the roughness of Type B and Type C of DMLS specimens is the same, the roughness of Type C specimen is a higher than Type B specimen produced by EBM.

If it is considered that the Type A is characterized essentially by the fully melted laser tracks that generate a primary roughness, Type B or Type C surfaces have a roughness due to the underlying primary roughness, see Fig. 3b, underneath a secondary roughness contribution due to partially melted particles. From inspection of Tab.1 and 2, the secondary roughness contributes about 10 μm to both DMLS and EBM measurements and possibly depends on the average particle size, while the primary roughness of EBM is about twice the primary roughness of DMLS.

The difference in primary and total roughness of Tab. 1 and 2 correlates with the fatigue data presented in the previous section showing a better performance of DMLS Ti6Al4V compared to the EBM Ti6Al4V. The directional effect in fatigue is quite limited for both the PBF processes and therefore at variance with the global surface roughness measurements. The concept of primary roughness could be a more representative indicator of surface quality in

fatigue, i.e. the primary roughness is the same for all three specimen directions for both PBF processes and it ranks DMLS better than EBM. Since standard surface roughness measures may not quantify the impact of as-built surface on fatigue, other parameters have been proposed and explored for example in [17].

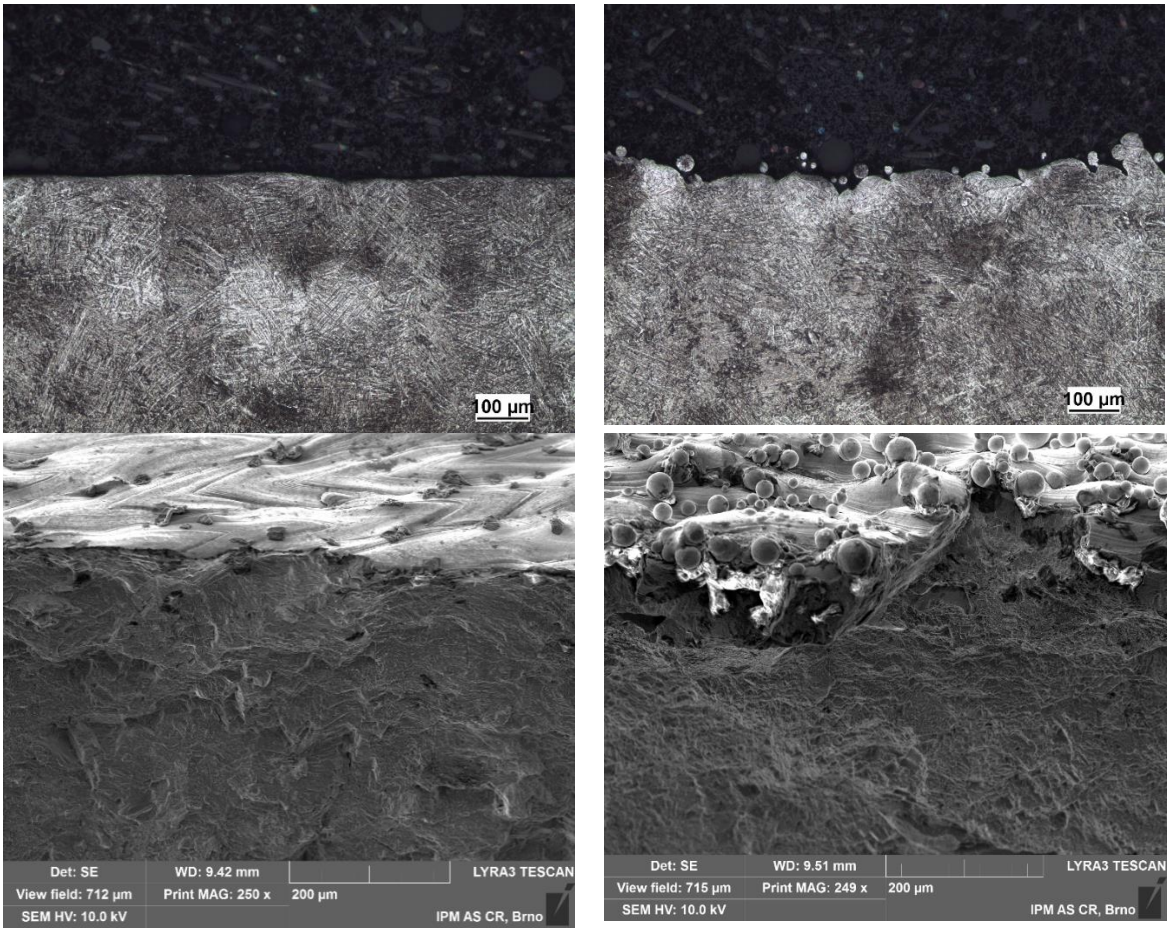

Fig. 7 DMLS roughness of planes under the loading Type A and C a) and b) longitudinal profile, OM; c) and d) fracture profile, cross section, SEM.

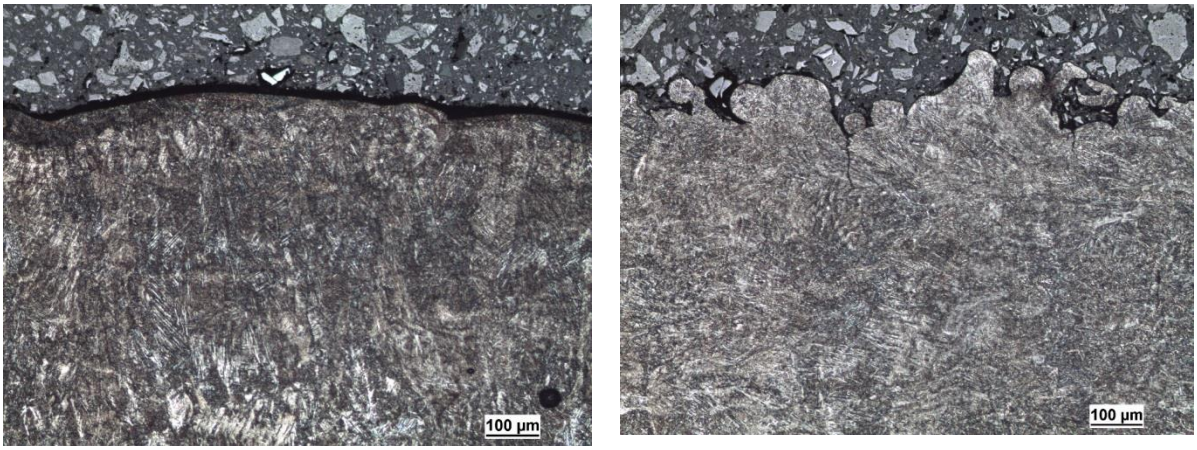

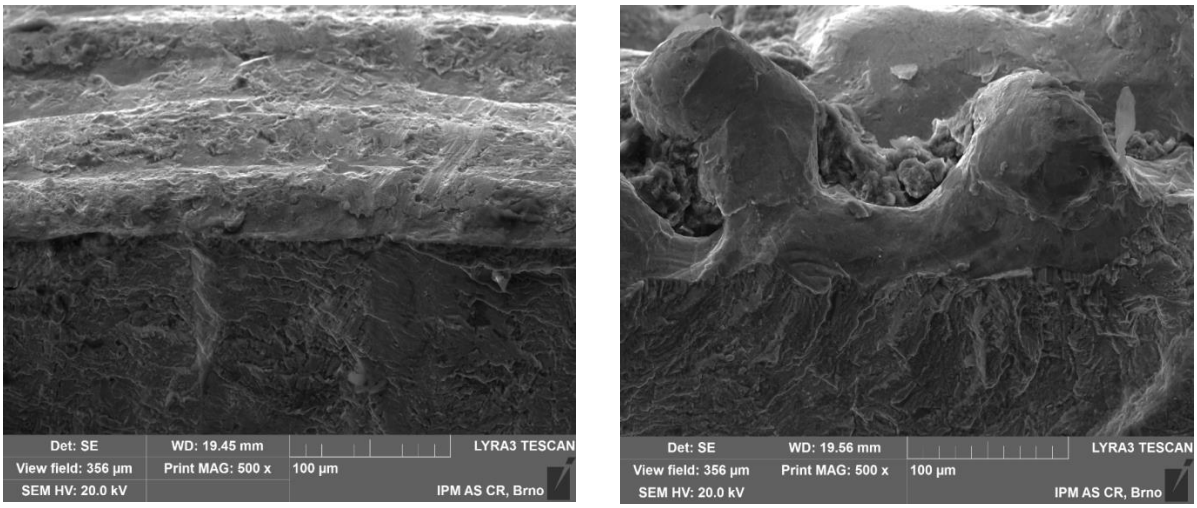

Fig. 8 EBM roughness of planes under the loading of Type A and C specimens a) and b) longitudinal profile, OM; c) and d) fracture profile, cross section, SEM.

Now, further insight could be gained examining the micrographs of Fig. 7 and 8. The longitudinal sections of Type A and of Type C specimens are shown in Fig.7a and 7b for DMLS Ti6Al4V and in Fig. 8a and 8b for EBM Ti6Al4V. The dramatic difference between the two surface morphologies already apparent from the respective roughness measurements is confirmed, although the differences do not impact significantly the respective fatigue response. An almost flat surface is characteristic of Type A DMLS specimens, Fig. 7a. The fatigue fracture surface is perpendicular to the applied stress and initiated at a surface irregularities visible in SEM image of Fig. 7c. The longitudinal profile of Type C DMLS specimens is characterized by the presence of sharp notches, Fig. 7b. Initiating cracks can form easily at notches as shown in SEM image of a fatigue fracture surface, Fig. 7d.

Fig. 8a shows a wavy surface of Type A EBM specimens, confirmed by the SEM view of a broken specimen in Fig. 8c. The longitudinal profile of Type C EBM specimens of Fig. 8b shows a surface with deep sharp notches with evidence of initiated cracks. Initiating cracks can form easily at notches as shown in SEM image of a fatigue fracture surface of Fig. 8d.

A final remark on Figs. 7 and 8 is the following. The top layer of as-built PBF surfaces is quite irregular and rough. So while local sub surface defects may have at times contributed to crack initiation, roughness-induced initiation without evidence of a starting defect was also frequent. A generalization on the role of defects on crack initiation is therefore difficult. On the other hand, recent studies on fatigue of machined specimens were able to demonstrate the influence on subsurface defects more clearly, [9, 10, 18].

4. DISCUSSION

This section begins with a validation by comparison of the present fatigue data in order of supporting the adoption of the non-conventional mini specimen geometry of Fig. 1. In [20] the data of the present test method were compared for example to rotating bending specimen data. The plot of Fig. 9 shows a comparison between rotating bending test results obtained with as-built standard 6-mm-dia vertical specimens and the present plane bending tests for the Type C specimens (i.e. vertical). The production of both types of specimen was according to the DMLS process specified before (i.e. same EOS system and same post fabrication heat treatment in vacuum). The definition of an equivalent stress amplitude for R = -1 according to the Haigh equation, [23], was used transform the present data obtained at R = 0 and allow a comparison with the stress amplitudes of rotating bending specimens (i.e. characterized by R = -1). A similar approach was used in [2] to compare different fatigue data at different load ratios taken from the literature and draw some general conclusions. Fig. 9 shows that the mini specimen data and standard specimen data reasonably correlate. The estimated fatigue strength at 2 106 cycles is 180 MPa for the mini specimens and 160 MPa for the rotating bending specimens. Therefore, the mini specimen geometry and test method can be reasonably used to explore the many factors affecting fatigue of PBF materials as done for example in [24].

To further assess the present fatigue data, Ref. [17] is used. A plane bending configuration was adopted to test and compare the EBM and the DMLS processes applied to the fabrication of Ti6Al4V. The approach involved fixing a common, rather high maximum stress of 600 MPa at R=0.1 (i.e. equivalent 570 MPa at R = 0) and determined the corresponding fatigue lives on multiple specimens. He determined a mean life of 28 961 cycles (standard deviation of 5 557 cycles) for EBM and a mean life of 62 133 cycles (standard deviation 8 323 cycles) for DMLS. If these data are inserted in the combined plot of Fig. 6 an excellent agreement is found for both PBF processes. Actually his scatter-band is also compatible with the present experimental scatter-band.

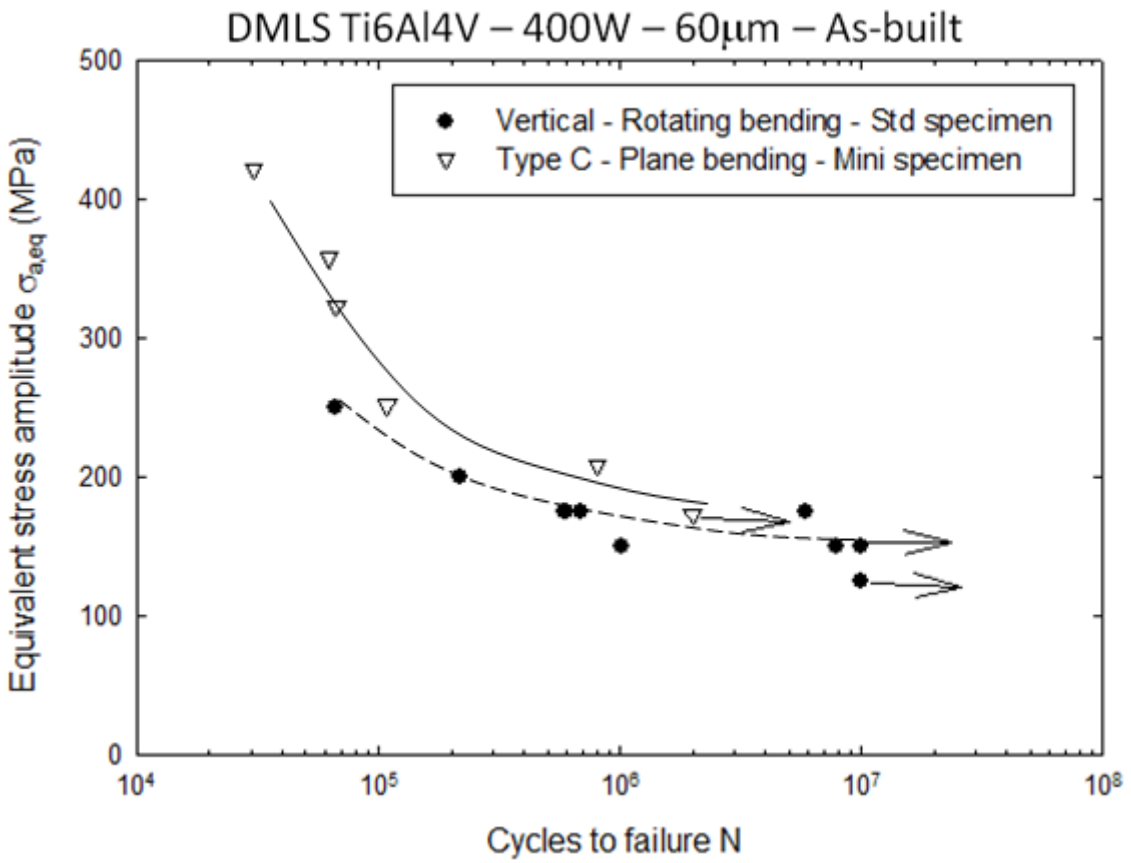

Fig. 9 Comparison of fatigue curves of as-built DMLS Ti6Al4V obtained using two different experimental methods: cyclic plane bending of mini specimens and rotating bending of standard specimens.

However, the fatigue testing of as-built PBF Ti6Al4V is most often performed according to the cyclic tension loading condition applied to specimens having the longitudinal axis parallel to build direction (i.e. vertical), for example [3,4,16,18]. This condition is expected to generate different results when compared to the cyclic bending loading condition. However, influence factors, such as different PBF processing methods as examined here, can be quantified and compared. Recently the influence of as-built surfaces on fatigue behavior of DMLS and EBM Ti6Al4V using smooth 5-mm-dia geometry in cyclic tension was studied in [16]. Being fatigue stress ratio R = 0.1, the max stress vs life data can be readily compared to the present plane bending 5 x 5 mm section and R = 0 since the effective max stress of [16] needed to be reduced by only by 4 %.

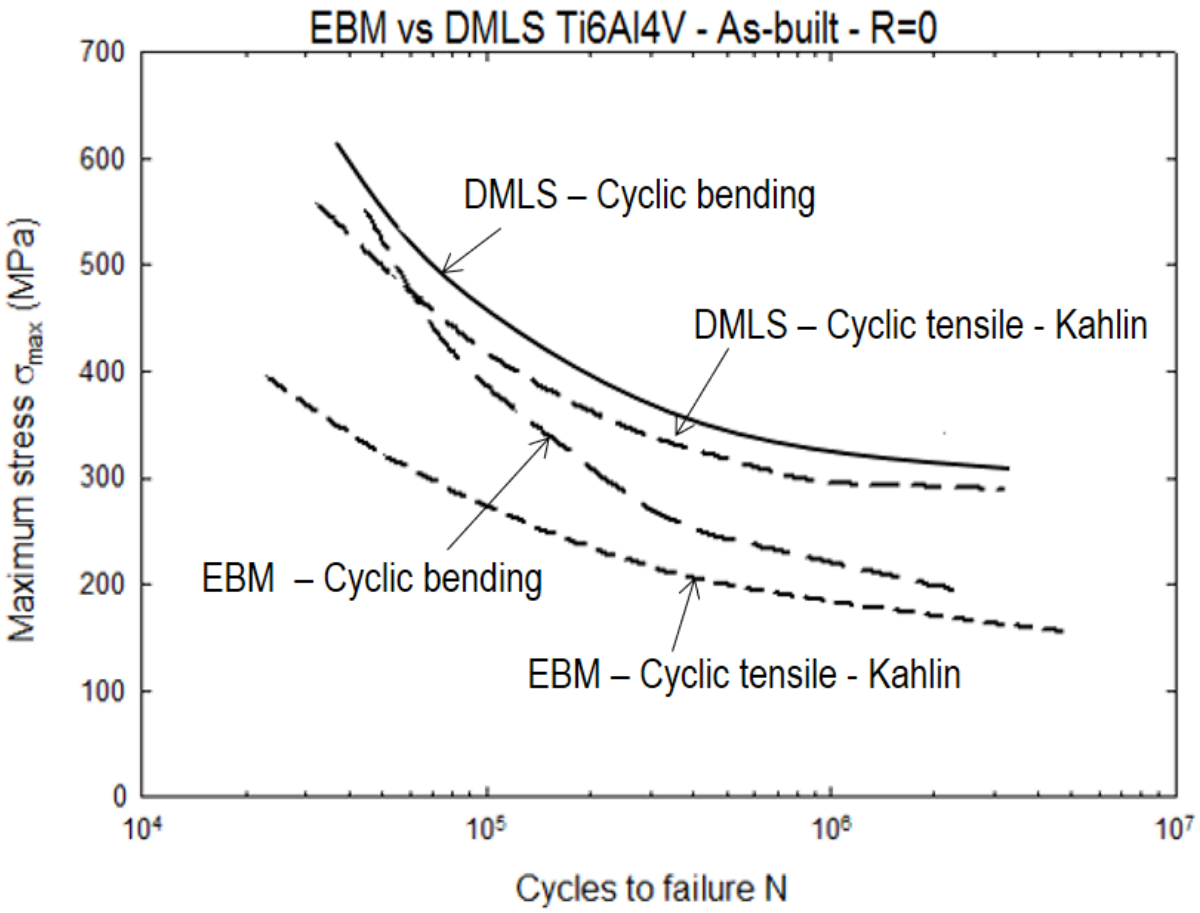

Fig. 10 Comparison of fatigue curves of as-built EBM vs DMLS Ti6Al4V obtained using two different experimental methods: cyclic tensile of standard specimens and cyclic bending of mini specimens.

Fig. 10 shows the mean fatigue curves of the scatter bands of Fig. 6 for EBM and DMLS obtained with the present experimental program along with the trend curves of fatigue tests reported in [16]. Testing of specimens under cyclic tensile loading confirm the ranking of the two PBF technologies obtained by testing mini specimen under cyclic plane bending. For a given PBF technology, cyclic tensile loading conditions determine slightly lower fatigue strengths compared to cyclic bending because of the role played by the different volume of highly stressed material activated by the specific loading mode. It is well accepted that a larger stressed volume reduces the measured fatigue strength for the potential defect content. Therefore, the as-built mini specimens of Ti6Al4V produced with both DMLS and EBM processes generate fatigue data coherent with the data from a standard test procedure when

specimens are produced with the same state-of-the-art technology. The fatigue performance of as-built EBM Ti6Al4V is confirmed inferior to that of the as-built DMLS Ti6Al4V.

Such PBF process ranking in fatigue appears qualitatively coherent with the interpretation that the surface roughness plays a major role in promoting early fatigue crack initiation. An assessment of the current roughness measurements of Tab. 1 and 2 is, however, in order because fatigue models have been proposed based on the role of surface roughness, [13, 17].

Recently Greitmaier et al. compared the high cycle fatigue behavior of DMLS and EBM specimens produced using industrial systems equivalent to those used in the present study, [13]. They measured a process-inherent surface roughness Ra = 13 μm for DMLS and Ra = 27 μm for EBM. When these measurements are compared with the data of Tab. 1 and 2, they are found to exactly match the surface roughness of the Type B and Type C specimens. This observation however open the question of why the significantly lower roughness of Type A specimens (i.e. Ra = 3.3 μm for DMLS and Ra = 7.3 μm for EBM) does not contribute to a significant life extension of the Type A specimens compared to the other two directions as shown in Fig. 4 and 5. A possible explanation is that the fatigue behavior, is controlled by the primary roughness present on the stressed surface of Type A specimens rather than the total, primary and secondary, roughness measured on the as-built surfaces perpendicular to the layers, (i.e. Type B and Type C specimens). Nonetheless, while the melt track width modulates the primary roughness of Type A specimens, the layer thickness may affect the Type C primary roughness. The fatigue strength at 10^7 cycles of DMLS and EBM Ti6Al4V cyclic tension specimens reported in [13] are significantly lower than the values reported here supported by Kahlin [16]. A possible size effect is expected when the different specimen geometries are compared. However, the relative fatigue performance FP of the PBF processes given by the FP(EBM)/FP(DMLS) ratio is similar: 0.67 from the present data vs. 0. 74 for [13].

Chan [17] performed ray microcomputed tomography (micro-CT) imaging to characterize the surface features of the as-built DMLS and EBM Ti6Al4V specimens. From measurements of depth and radius of the surface notches the corresponding elastic concentration factors were computed: K_t of the surface notches in the DMLS material was lower than in the case of EBM material (i.e. 2.31 vs 3.28 respectively), [17]. Not unexpectedly, the severity of the surface features correlates to the fatigue life properties of the PBF alloy. The surface roughness was then examined and the mean and the maximum values of the surface valley depth, Rvi rather

than the mean Ra as in Tab. 1 and 2 was proposed as characterizing parameter. According to [17], the fatigue performances of the as-built EBM and DMLS Ti6Al4V is a long fatigue crack growth phenomenon because there are surface notches with depths that are larger than the material intrinsic parameter, [25].

5. CONCLUSIONS

Smooth fatigue behaviour of heat treated DMSL Ti6Al4V and EBM Ti6Al4V has been determined using miniature specimens having different orientations with respect to build direction. The results have been discussed on the basis of the as-built surface characterization and of previous studies on the same material and processes from the literature.
The following conclusions are reached:

- The fatigue strength of as-built DMSL Ti6Al4V is significantly higher than that of as-built EBM Ti6Al4V.
- The surface roughness of DMSL Ti6Al4V is considerably lower than that of EBM Ti6Al4V.
- Relevant studies from the literature confirm both the previous conclusion.
- The directional fatigue data show slight differences among them for either technology while the directional surface roughness measurements and morphology are significantly different.
- Only the primary roughness related to the process parameters and not the secondary roughness due to the partially melted powder particles may contribute to the fatigue behaviour of as-built Ti6Al4V.
- The new fatigue test methodology using mini specimens in cyclic plane bending conveniently provides original information on the behaviour of as-built PBF metals.
- The fatigue data obtained with the new methodology are coherent with data obtained by standard (i.e. large volume) specimens and test methods.

ACKNOWLEDGEMENTS

The research was partially supported by the project Slovak VEGA grant No. 1/0685/2015. Specimen production by partner company BEAM-IT srl, Fornovo Taro, Italy is acknowledged with thanks. L. Cassi tested part of the EBM specimens for his thesis work.

REFERENCES

[1] Bandyopadhyay, A., Bose, A. Additive manufacturing: Additive manufacturing technologies of metals using powder-based technology. Taylor & Francis Group: Boca Raton, (2016) 377.

[2] Li, P., Warner, D.H., Fatemi, A., Phan, N. Critical assessment of the fatigue performance of additively manufactured Ti–6Al–4V and perspective for future research, Int J Fatigue, 85 (2016).

[3] Edwards, P., Ramulu, M. Fatigue performance evaluation of selective laser melted Ti–6Al–4V. Mater. Sci. Eng. A, (2014) A598, 327–337.

[4] Mower, T. M., Long, M. J., 2016. Mechanical behavior of additive manufactured, powder-bed laser-fused materials. Materials Science and Engineering, A651 198-213.

[5] Kranz, J., Herzog, D., Emmelmann, C. Design guidelines for laser additive manufacturing of lightweight structures in TiAl6V4. J Laser Appl (2015); 27: S14001.

[6] Kruth, J.P., Levy, G., Flocke, F., Childs, T.H.C. Consolidation phenomena in laser and powder-bed based layered manufacturing, Ann. CIRP 56(2) (2007) 730–759.

[7] Gong, H., Rafi, K., Starr, T., Stucker, B. The effects of processing parameters on defect regularity in Ti-6Al-4V parts fabricated by selective laser melting and electron beam melting, 24th Annual International Solid Freeform Fabrication Symposium, (2013) 424-439.

[8] Wycisk, E., Solbach, A., Siddique, S., Herzog, D., Walther, F., Emmelmann, C. Effects of defects in laser additive manufactured Ti–6Al–4V on fatigue properties. Phys. Proc, (2014) 56, 371–378.

[9] Liu, Q., Elambasseril, J., Sun, S., Leary, M., Brandt, M., Sharp, P.K. The effect of manufacturing defects on the fatigue behavior of Ti–6Al–4V specimens fabricated using selective laser melting, Adv. Mater. Res. 891–892 (2014) 1519–1524.

[10] Hrabe, N. et al. Fatigue properties of a titanium alloy (Ti–6Al–4V) fabricated via electron beam melting (EBM): Effects of internal defects and residual stress. Int J Fatigue (2016), http://dx.doi.org/10.1016/j.ijfatigue.2016.04.022

[11] Kasperovich, G., Hausmann, J. Improvement of fatigue resistance and ductility of TiAl6V4 processed by selective laser melting. J Mater Process Technol (2015) 220:202–14.

[12] Chan, K.S., Koike, M., Mason, R.L., Okabe, T. Fatigue life of titanium alloys fabricated by additive layer manufacturing techniques for dental implants, Metall. Mater. Trans. A44A (2013) 1010–1022.

[13] Greitemeier, D., Dalle Donne, C., Syassen, F., Eufinger, J., Melz, T. Effect of surface roughness on fatigue performance of additive manufactured Ti–6Al–4V. Materials Science and Technology. (2015) 629-634.

[14] Bača, A., Konečná, R., Nicoletto, G., Kunz, L., Effect of surface roughness on the fatigue life of laser additive manufactured Ti6Al4V alloy. Manufacturing technology, 15 (4) (2015), 498-502.

[15] Bagehorn, S., Wehr, J., Maier, H.J. Application of mechanical surface finishing processes for roughness reduction and fatigue improvement of additively manufactured, International Journal of Fatigue 102 (2017) 135–142.

[16] Kahlin, M., Ansell, H., Moverare, J.J. Fatigue behaviour of notched additive manufactured Ti6Al4V with as-built surfaces, Int J Fatigue 101 (2017).

[17] Chan, K. S. Characterization and analysis of surface notches on Ti-alloy plates fabricated by additive manufacturing techniques. Surf Topogr Metrol Prop 3: 44006 (2015).

[18] Greitemeier, D., Palm, F., Syassen, F., Melz, T. Fatigue performance of additive manufactured TiAl6V4 using electron and laser beam melting. Int J Fatigue (2017); 94:211–7.

[19] Konečná, R., Nicoletto, G., Bača, A., Kunz, L., Metallographic characterization and fatigue damage initiation in Ti6Al4V alloy produced by direct metal laser sintering. Materials Science Forum, Vol. 891, (2017) 311-316.

[20] Nicoletto, G. Anisotropic high cycle fatigue behavior of Ti-6Al-4V obtained by powder bed laser fusion. International Journal of Fatigue, 94, (2017) 255-262.

[21] Bača, A., Konečná, R., Nicoletto, G., Kunz, L. Influence of build direction on the fatigue behaviour of Ti6Al4V alloy produced by direct metal laser sintering. Materials Today: Proceedings 3, (2016) 921-924.

[22] ASTM F2924-14, Standard Specification for Additive Manufacturing Titanium-6 Aluminum-4 Vanadium with Powder Bed Fusion, ASTM International, West Conshohocken, PA, 2014, www.astm.org.

[23] Juvinall, R., Marshek, K.M., 2012. Fundamentals of Machine Component Design, New York: John Wiley, 929.

[24] Nicoletto, G., Directional and notch effects on the fatigue behavior of as-built DMLS Ti6Al4V, International Journal of Fatigue, 106, (2018), 124-131.

[25] Nicholas, T. High cycle fatigue: a mechanics of materials perspective, Elsevier; 2006.